

## Experimental Study of Forced Convection Heat Transfer Porous Media inside a Rectangular Duct at Entrance Region

Moayed R.Hasan

*Mechanical Engineering Department, University of Technology, Baghdad-Iraq*

Suhad A.Rasheed

*Mechanical Engineering Department, University of Technology, Baghdad-Iraq*

[Sah\\_Jumaily66@yahoo.com](mailto:Sah_Jumaily66@yahoo.com)

Ali Najeh Mahdi

*Mechanical Engineering Department, University of Technology, Baghdad-Iraq*

[alinajeh999@gmail.com](mailto:alinajeh999@gmail.com)

Submission date:- 17/12/2018	Acceptance date:- 30/1/2019	Publication date:-7/2/2019
------------------------------	-----------------------------	----------------------------

### Abstract

This work presents experimental investigation of flow and heat transfer characteristics for entry length of turbulent flow in a rectangular duct fitted with porous media and air as the working fluid. Rectangular duct (300×30 mm) with a hydraulic diameter (54.54 mm) was subjected to constant heat flux from lower surface ( $1.5 \times 10^2 - 1.8 \times 10^2 \text{ w/m}^2$ ) and Reynolds number ranged ( $3.3 \times 10^4$  up to  $4.8 \times 10^4$ ). Copper mesh inserts (as porous media) with screen diameter (54.5 mm) for vary distance between two adjacent screens of (10 mm), (15 mm) and (20 mm) in the porosity range of (0.98 - 0.99) are considered for experimentation. The effect of porous height ratio (full and partial) are also considered. It is observed that the enhancement of heat transfer by using mesh inserts when compared to a plain surface is more by a factor of (2.2) times where the skin friction coefficient is about (5) times. An Empirical correlation for Nusselt number and friction factor are developed for the mesh inserts from the obtained results.

**Keywords:** Forced convection, Porous media, Wire mesh, Nusselt number, Friction factor.

Character	Description	Units
$A_c$	Cross-sectional area (H.W)	$m^2$
AR	Aspect ratio	-
b	Half duct height (H/2)	m
$C_p$	Specific heat at constant pressure	$kJ/kg.K$
$C_f$	skin friction coefficient	-
$D_h$	Hydraulic diameter	m
f	Friction factor	
g	Acceleration due to Gravity= 9.81	$m/s^2$
H	Duct height	m
h	local heat transfer coefficient	$W/m^2.K$
I	Current	A
k	Thermal conductivity	$W/m.K$
L	Length	m
$\dot{m}$	Mass flow rate	$kg/s$
P	Pressure	$N/m^2$
Q	Rate of heat	W
q	Heat Flux	$W/m^2$
$T_w$	Surface temperature	K
$T_a$	Ambience Temperature	K
$T_i$	Local Temperature	K
$u_b$	Bulk velocity	$m/s$
V	Voltage	Volt
W	Duct width	m
$\rho$	Density of Air	$kg/m^3$
$\tau$	Averaged Viscous Shear Stress	$N/m^2$

## 1. Introduction

The introduction of porous media inform of mesh wire for heat transfer enhancement is found in numerous applications, e.g, electronic cooling, drying processes, a solid matrix, heat exchangers and enhanced recovery of petroleum reservoirs. The using of porous has proved to be very promising in heat transfer enhancement. One of the important porous media characteristics is represented by an extensive contact surface between solid and fluid surface. The large contact surface enhances the internal heat exchange between the phases and consequently results in an increased thermal diffusivity [1].

The flow in a duct can be divided in two parts: boundary flow (which represents a boundary layer in the entrance length and on the fluid layer near a wall in the fully developed) and core flow. The commonly used methods in the boundary layer flow are :(a) disrupting the fluid boundary layer near the wall, (b) extending the solid surface to enhance heat transfer, (c) changing the chemical and physical nature of the surface. This method causes enhancement in the boundary flow. Boundary flow methods also increase the flow resistance, as the velocity gradient, viscous diffusion and the momentum loss of fluid near the boundary increases, sharing strength and friction between the fluid and boundary may have different extents of growth [2]. In the core flow, heat transfer enhancement can be obtained without increasing too much flow resistance [3]. The more direct way is to make temperature as uniform as possible in the core flow in order to form a thin thermal boundary layer near the wall with great temperature gradient, not increase velocity gradient in the flow filled ,not to disrupt fluid near the boundary layer and not to extend continuous surface on the wall [2].

Liu et al. [4] introduced the principles of enhanced heat transfer in the core flow to form an equivalent thermal boundary layer in the fully developed laminar tube flow. The numerical results show that the porous media filled in the fully developed laminar tube flow should be high thermal conductivity, high porosity and high porous ratio. When thermal conductivity, porosity and porous radius ratio of the porous material were 200 w/m.C, 0.92 and 0.96 respectively, the performance evaluation criteria [PEC] values were 3 and 2.5 for air and water respectively. Based on the concept of enhanced heat transfer in the core flow.

Huang et al. [5] investigated experimentally and numerically the flow resistance and heat transfer characteristics of the air flow for laminar to fully turbulent ranges of Reynolds numbers. The obtained results show that the heat transfer rate of the tube with porous inserts whose diameters approach the diameter of the tube is about 1.6 – 5.5 times larger than the smooth tube cases in laminar, transitional and turbulent ranges of Reynolds number. The experimental results of [PEC] indicated that the method has good integrated performance of the heat transfer enhancement in the laminar flow where the [PEC] values are larger than unity with the maximum value of about 1.44 obtained at  $Re=1000$  and porosity ( $\epsilon=0.951$ ). The results showed a good agreement between experimental and numerical work.

Kurian et al. [6] investigated experimentally the hydrodynamic and thermal performance of stainless steel wire (as porous media) blocks in a vertical channel for different aspect ratio. In this work, stainless steel wire mesh was arranged side by side to act as porous block. Convective heat transfer experiments in a vertical channel using an isothermal flat plate were considered for Reynolds showed that, Colburn J factor was increased by almost two times as compared to clear channel case for Reynolds number. It was observed that the friction factor and Colbrun J factor increased with the mesh block thickness. Based on the experimental results a correlation for a Nusselt number with Reynolds number and channel aspect ratio had been developed.

Siva M. et al. [7] studied experimentally heat transfer performance for forced convection of water in a horizontal pipe partially filled with a porous media. The porous inserts used in this study was made of packed steel balls. The obtained results showed that maximum augmentation in heat transfer with minimum pressure drop was observed for a core of diameter 55mm with porosity 0.44, which was around 4.6 times higher as compared to the plain tube.

H. Shokouhmand et al. [8] studied the effect of porous insert position on enhanced heat transfer in a parallel- plate channel partially with a fluid-saturated porous medium. In this study, laminar flow and convective heat transfer in duct partially filled with a porous medium were investigated numerically. The porous inserted in the core and near the walls at constant wall temperature. It was found out that with a porous layer located in the channel core, pressure loss was higher than that of the case with porous medium adjacent to the walls.

Hussain et al. [9] the local wall temperature regularly increases with the flow direction, diminishes with the Reynolds number and increments with warmth motion, yet the fluid temperature continuously diminishes in the permeable medium with the vertical bearing far from the warmed wall, and the results demonstrate an expansion in local Nusselt.

Pastore et al. [10] the conduct of two porous media with different grain sizes and specific surfaces has been watched. The understanding of the experimental data shows that the heterogeneity of the porous medium affects heat transport dynamics, causing a channeling effect, which has consequences on thermal dispersion phenomena and heat transfer between fluid and solid phases, restricting the ability to store or disperse heat in the porous medium.

It is worth mentioning that the number of numerical investigation in the field of inserting porous media is large compared to the number of experimental studies especially in the entry length of turbulent flow. In addition, most of the flow problem in industrial the heat exchangers involve turbulent flow region and there usually exists an entrance region in each tube of heat exchanger.

The aim of the present experimental investigation is to demonstrate the effect of inserting copper mesh (as porous media) in the porosity (0.98 – 0.99) on the heat and flow characteristics in the entry length of turbulent flow at Reynolds numbers range ( $3.3 \times 10^4$  up to  $4.8 \times 10^4$ ). The effect of porous height ratio (core and boundary flow) is also considered. Experiments are conducted at constant heat flux range ( $1.5 \times 10^2$  –  $1.8 \times 10^2$  w/m<sup>2</sup>) in rectangular duct (300×30 mm) when  $Dh=54.5$  mm.

## 2. Experimental Apparatus and Procedure:

The schematic and photograph of the experimental rig are shown in fig.(1) and fig.(2) respectively. The experimental rig is an open-circuit blower fan by forced air to the duct. The test channel had the rectangular cross section of 300mm (width) by 30mm (height). The channel (duct) consisted of the inlet

sectional (750mm), test section (400mm) and exit section (1250mm). The channel aspect ratio is (10:1) and hydraulic diameter (54.54mm). The channel was manufactured by using 20mm thick plywood. While, a (7mm) thick heated the aluminum plate was used to manufacture the lower surface of the channel. To obtain constant heat flux electric wire with high resistance wrapped (1mm) thick mica, which was sandwiched between two another 0.5mm thick mica layers as shown in fig(3). The heater assembly glued to the lower surface of channel. The rear side of the heater assembly was thermally insulated to transfer as much as possible of the heat generated by a heater to the airflow. Electric power was supplied through variac transformer to obtained required heat flux voltmeter and an ammeter were used to measure voltage and current respectively. The distance from the inlet of the duct to test section is (30×30 cm) with 40cm length. All measurements for plain and porous duct were carried out at this section. The porous media used for the experimental are the copper screen (wire diameter 0.5 mm). Fig (4) illustrates a schematic of the test section where wire mesh is arranged. The porosity of porous media was defined according to the distance between two adjacent screens.

Thermocouples k-type were used to measure temperatures. For measuring the wall temperature small holes were drilled (4 mm). Thermocouples were inserted into these holes, and they were fixed with special material. The selector switch was used to toggle between thermocouples and the output displayed on a temperature indicator. To measure bulk air temperature special mechanism was selected to obtain local air temperature in the (y-z) plane at any stream wire direction. From this mesh reading, the bulk air temperature obtained.

Static pressure taps were distributed at the upper surface in streamwise and spanwise directions. Local and average air velocity was calculated at any section in streamwise and spanwise directions with Pitot tube (total pressure) and adjacent static pressure tapping, using micromanometer.

Preston tube was linked to micromanometer and from the obtained reading. The value of skin friction coefficient can be calculated as explain later.

### 3. Operating procedure and data reduction:

Air at ambient temperature from the room was forced through the inlet section and entered the duct by a centrifugal blower. The mass flow rate was controlled by adjusting a sliding gate sited at the exit of a blower. After the airflow was adjusted to a prescribed velocity, the current was supplied to the heater.

The heat flux was selected so the surface temperature was maintained within the permissible region of duct material. Once the steady state condition was reached, the heat flow measurements were recorded.

$$\dot{m} = \rho_a u_b A \quad \dots (1)$$

The Reynolds number was introduced by the following equation:

$$Re = \frac{D_h u_b}{\nu} \quad \dots (2)$$

Also can be calculated by using the following relation:

$$D_h = \frac{4A}{P_w} = \frac{4(H \times W)}{2(H+W)} \quad \dots (3)$$

The wall shear stress and skin friction coefficient in the test section for plain and porous surface were calculated according to the following equations:

$$\tau_w = -\frac{H}{2} \times \frac{dp}{dx} \quad (\text{Smooth surface}) \quad \dots (4)$$

While for porous media, friction factor was determined from the measured value of dynamic pressure (by Preston tube) at using the equation Head and Ram [11]:

$$a - y^* = 0.5x^* + 0.037 \quad \dots (5)$$

$y^* < 1.5$ , and  $u_r d / 2\nu < 5.6$

$$b- y^*=0.8287-0.1381x^*+0.1437x^{*2}-0.006x^{*3} \quad \dots (6)$$

1.5 < y\* < 3.5 and 5.6 < u<sub>t</sub>d/2ν < 55

$$c- x^*=y^*+2 \log_{10} (1.95y^*+4.1) \quad \dots (7)$$

3.5 < y\* < 5.3 and 55 < u<sub>t</sub>d/2ν < 800

$$x^* = \log_{10} \left[ \frac{\Delta p d^2}{4 \rho_a \nu^4} \right] \quad \dots (8)$$

$$y^* = \log_{10} \left[ \frac{\tau_w d^2}{4 \rho_a \nu^4} \right] \quad \dots (9)$$

The friction coefficient was calculated for plain and porous surface from the following equation:

$$C_f = \frac{\tau_w}{\frac{1}{2} \rho_a u_b^2} \quad \dots (10)$$

The sensible heat gained by air can be calculated using relation:

$$Q_a = \dot{m} C_p (T_{out} - T_{in}) \quad \dots (11)$$

In addition, the heat balance can be checked by comparing Q with the exterior heat input to air Q<sub>e</sub>=I.V ... (12)

The heat balance errors of all experiment results were limited to less than (2%) and the heat loss rate by radiation and condition through the insolation were estimated.

The local heat transfer coefficient was calculated according to the following relationship:

$$h = \frac{q_{con}}{A (T_w - T_b)} \quad \dots (13)$$

The Nusselt number was introduced by the following equation:

$$Nu = \frac{h D_h}{K_e} \quad \dots (14)$$

The effective thermal conductivity of a fluid filled porous media calculated by the following relationship [12]:

$$k_e = k_a^\epsilon k_p^{(1-\epsilon)} \quad \dots (15)$$

The thermal performance criteria (PEC) was evaluated by the following equation [13]:

$$PEC = \frac{Nu_p / Nu_s}{(Cf_p / Cf_s)^{1/3}} \quad \dots (16)$$

The uncertainty analysis was performed by applying the estimation method proposed by Hugh W. et al. [14]. The uncertainty in local Nusselt and local friction factor values were estimated to be 6.91% and 0.45% respectively.

#### 4. Validation of Experimental Data

The validation of experimental results is first validated in terms of Nusselt number and friction factor obtained from the present smooth channel compared with the correlations in the open literature. For turbulent flow, the correlation of friction factor for a smooth rectangular duct was given by the modified Blasius equation: f=0.085Re<sup>-0.25</sup>[15]. The average deviation between the predicted and experimental values has been found to be 7.7-8.5% as shown in fig (5). The Nusselt number for a smooth rectangular duct is given by the Dittus-Boelter equation [Nu =0.023Re<sup>0.8</sup>Pr<sup>0.4</sup>] [15]. The comparison of the experimental and predicted values Cf as a function of Reynolds number is shown in fig (6) .The average deviation between the predicted and experimental values has been found to be 18-21 %. This shows a good match between the two values, which ensures the accuracy of the experimental data with the present experimental set-up. Thus, a reasonably

good agreement between the two sets of values ensures the accuracy of the data being collected using this experimental setup.

## 5. Results and Discussion

### 5.1. Flow characteristics for Plain and Porous Media:

Fig (7 and 8) present the dimensionless velocity profile in the entry region for clear flow and porous cases at  $ReDh=4.8 \times 10^4$  and  $ReDh=3.3 \times 10^4$

It is clear that the existence of porous media leads to shifting the maximum velocity toward the duct wall. In general, the velocity profile deformed in compared with clear flow. As a result, speed tendency closes the wall channel as matched with pure flow case as was reported Bogdan I. et al. [10]. Variation of Reynolds number does not change the behavior of velocity profile.

Fig (9) depicts the local skin friction coefficient for clear and porous cases. As a result of increasing surface area with the existence of porous media and the deformation of velocity profile the pressure drop increases in the porous case. Therefore, the skin friction increased. This figure illustrates that skin friction coefficient increases with decreasing porosity, which can be attributed to the same above reasons. These figures show that the increase of skin friction coefficient for clear flow in the entrance region is very slowly, while for porous flow is very sharp especially behind the porous media. The maximum increase in skin friction coefficient values is about (9 times) at  $\epsilon=98\%$ .

Fig (10) reveals the effect of porous material radius average  $R_p$  in skin friction coefficient. The increasing in  $R_p$  leads to increase  $C_f$ . As expected, the largest occupied with porous media. Surely, increase  $R_p$  associated with increasing surface area, so increasing pressure drop.

The influence variation Reynolds no. On the skin friction coefficient to the clear and porous cases are shown in fig (11).

It is clear that ordinary behavior was achieved for clear and porous cases. The skin friction coefficient decreases with increasing Reynolds number. For porous media, the variation of porosity does not change the general behavior.

### 5.2. Heat Transfer Characteristics for Plain and Porous Media:

Fig (12) shows the variation of air temperature recorded for clear and porous cases at specified Reynolds number and heat flux and various porosity. As is well known, porous media enhances heat transfer process by creating a complex flow filed inducing turbulence and increase significantly thermal conductivity. Therefore, this figure reports the increasing of air temperature as compared with a clear case. As porosity decreases, air temperature attained higher value. This attributed to a rise in the surface area and turbulence intensity.

The influence of radius ratio ( $R_p$ ) on variation the bulk temperature of air illustrate in fig (13). Inspection of this figure reveals that fully filling the duct with porous the medium ( $R_p=1$ ) gives higher air temperature compare with partial filling ( $R_p<1$ ). It is because that the larger thermal conductivity and larger surface area obtained.

Fig (14) depicts the effect of variable heat flux on bulk streamwise air temperature. The trends are very similar. The influence of variation Reynolds number on the bulk temperature air for clear and porous cases shown in fig (15).

Fig (16) depicts the variation of the local heat transfer coefficient for clear and porous cases. It is clear that using porous media leads to increase local heat transfer coefficient. The higher increasing obtained when porosity ( $\epsilon$ ) decreases.

These might be attributed to a complex flow filed inducing separation, recirculation and restarting the turbulent boundary layer as explained previously. Inspecting the trend of variation in this figure, the values of heat transfer coefficient after the first three locations were decreased gradually. While, at the last location

the heat transfer coefficient was decreased sharply and start to approach the value of clear case, diminishing influence of the porous (the point located after the last screen layer).

Fig (17) illustrates the effect of the ratio of porous media on heat transfer coefficient. It was shown that as ( $R_p$ ) increases the values of heat transfer coefficient are also increasing. This might be attributed to increase turbulence created as  $R_p$  increases. The local maximum enhancement occurs when  $R_p=1$  and  $\epsilon=0.98$  and is around 1.60 times when compared to clear case.

Fig (18) reports the effect of variation heat flux on the enhancement in heat transfer coefficient. It is clear that the percentage of enhancement increases with heat flux.

Fig (19) illustrates the variation of the local heat transfer coefficient with Reynolds number. It is clear that higher percentage enhancement occurs at lower Reynolds number.

Fig (20 and 21) shows the variation of local Nusselt number with Reynolds number in the streamwise direction. The local heat transfer coefficient distributions determine the trend of local Nusselt number, as explained above. Moreover, the Nusselt number enhancement is more pronounced at the smallest Reynolds number.

### 5.3. Thermal performance:

Fig (22) shows the variation of thermal performance with Reynolds numbers at different values of  $R_p$ . It can be seen that PEC decreases with increasing  $Re$  and it is generally above unity. Partial fill at  $R_p=0.8$  gives the highest value of PEC for all values of  $Re$ . Fig (23) reports the effect of porosity ( $\epsilon$ ) on (PEC) and it is shown that lower porosity gives the higher PEC regardless of Reynolds number. Fig (24) depicts the effect of heat flux on (PEC) and it was shown that increasing heat flux leads to increase (PEC) for all values of Reynolds number.

### 5.4. Correlations for Present Experimental Data:

Regression analysis was used to develop a relationship between Nusselt number, friction factor and Reynolds number that cover all combination of porosity ( $\epsilon$ ), radius ratio ( $R_p$ ) and the flow parameters for the entrance region.

The obtained correlation for Nusselt can be written as

$$Nu = 3.67(Re)^{-0.41} \epsilon^{-19.56} R_p^{0.3} \text{----- (17)}$$

A comparison between the experimental and predicted values of Nusselt number is shown in figure (25). The average deviation is about ( $\pm 6.5\%$ )

The obtained correlation for fraction factor can be written as,

$$f = 0.35 (Re)^{-0.22} \epsilon^{-34.04} R_p^{1.89} \text{----- (18)}$$

Fig (26) depicts comparison between the experimental data of fraction factor and those predicted from eq. (18). The average deviation is about ( $\pm 4.9\%$ )

### 6. Conclusions:

1. Using mesh wire in the entrance region leads to increase skin friction coefficient. The maximum increasing is about 9 times and occurred at lower porosity and when insert mesh wire as fill fulling ( $R_p=1$ ).
2. Porous media caused deformation of velocity profile and as a result, the maximum velocity was shifted towards the duct wall.
3. The enhancement values increasing with heat flux, porosity, radius ratio ( $R_p$ ) and decreasing Reynolds number.
4. The performance evaluation criteria (PEC) for entrance region decreased with Reynolds number and it is greater than unity for all range of  $Re$ , heat flux,  $R_p$  and porosity.
5. Using partial fulling ( $R_p=0.8$ ) gave the higher value of PEC for both regions. This value increased with increasing heat flux and decreasing porosity ( $\epsilon$ ).

6. Empirical correlation were obtained depending on the geometry of porous media and flow parameters

#### CONFLICT OF INTERESTS.

- There are no conflicts of interest.

#### References

- [1] Naga Sarada S., Kalyani K. Radha and A. V. S. Raju, "EXPERIMENTAL INVESTIGATIONS IN A CIRCULAR TUBE TO ENHANCE TURBULENT HEAT TRANSFER USING MESH INSERTS", *ARPN Journal of Engineering and Applied Sciences*, VOL. 4, NO. 5, JULY 2009.
- [2] Bejan, A., "Convection Heat Transfer, Wiley", New York, 1984.
- [3] W. Liu and K. Yang, "Mechanism and numerical analysis of heat transfer enhancement in the core flow along a tube", *Sci. China, Series E*, vol. 51, pp. 1195-1202, 2008.
- [4] W. Liu, K. Yang<sup>1</sup>, Z.C. Liu<sup>1</sup>, T.Z. Ming<sup>1</sup>, A.W. Fan<sup>1</sup>, C. Yang, "Mechanism of Heat Transfer Enhancement in the Core Flow of a Tube and Its Numerical Simulation", *The Open Transport Phenomena Journal*, vol.2, pp. 9-15, 2010.
- [5] Z.F. Huang a, A. Nakayama b, K. Yang a, C. Yang a,b, W. Liu, "Enhancing heat transfer in the core flow by using porous medium insert in a tube", *International Journal of Heat and Mass Transfer*, vol. 53, pp. 1164–1174, 2010.
- [6] Kurian, Renju, C. Balaji, and S. P. Venkateshan. "Experimental investigation of convective heat transfer in a vertical channel with brass wire mesh blocks." *International Journal of Thermal Sciences* 99, 2016: 170-179.
- [7] Aa, Siva Murali Mohan Reddy, and Venkatesh M. Kulkarnib. "An Experimental Investigation of Heat Transfer Performance for Forced Convection of Water in a Horizontal pipe partially filled with a Porous Medium." 2016.
- [8] Shokouhmand, H., F. Jam, and M. R. Salimpour. "The effect of porous insert position on the enhanced heat transfer in partially filled channels." *International Communications in Heat and Mass Transfer* 38.8, 2011: 1162-1167.
- [9] Hussain, Ihsan Y., and Aya A. Yaseen. "An Investigation into Forced Convection Heat Transfer through Porous Media." *International Journal of Computer Applications* 66.1, 2013.
- [10] Pastore, Nicola, et al. "Experimental study of forced convection heat transport in porous media." *Nonlinear Processes in Geophysics* 25.2, 2018: 279-290.
- [11] D.H. Fefriss, "Preston Tube Measurements in Turbulent Boundary Layers and Fully Developed Pipe Flow", LONDON: HER MAJESTY'S STATIONERY OFFICE, 1965.
- [12] Bogdan I. Pavel, Abdulmajeed A. Mohamad, "An experimental and numerical study on heat transfer enhancement for gas heat exchangers fitted with porous media", *International Journal of Heat and Mass Transfer*, vol. 47, pp. 4939–4952, 2004.
- [13] Karwa, R., Sharma, C., & Karwa, N. Performance evaluation criterion at equal pumping power for enhanced performance heat transfer surfaces. *Journal of Solar Energy*, 2013.
- [14] Coleman H. W. and Steele W.G." Experimentation and Uncertainty Analysis for Engineers" John Wiley and Sons Inc. Second Edition, 1999 New York.
- [15] S. S. Pawar<sup>1</sup>, Dr. D. A. Hindolia<sup>2</sup>, Dr. J. L. Bhagoria, "Experimental study of Nusselt number and Friction factor in solar air heater duct with Diamond shaped rib roughness on absorber plate", *American Journal of Engineering Research (AJER)* e-ISSN : 2320-0847 p-ISSN : 2320-0936 Volume-02, Issue-06, pp-60-68, 2013.



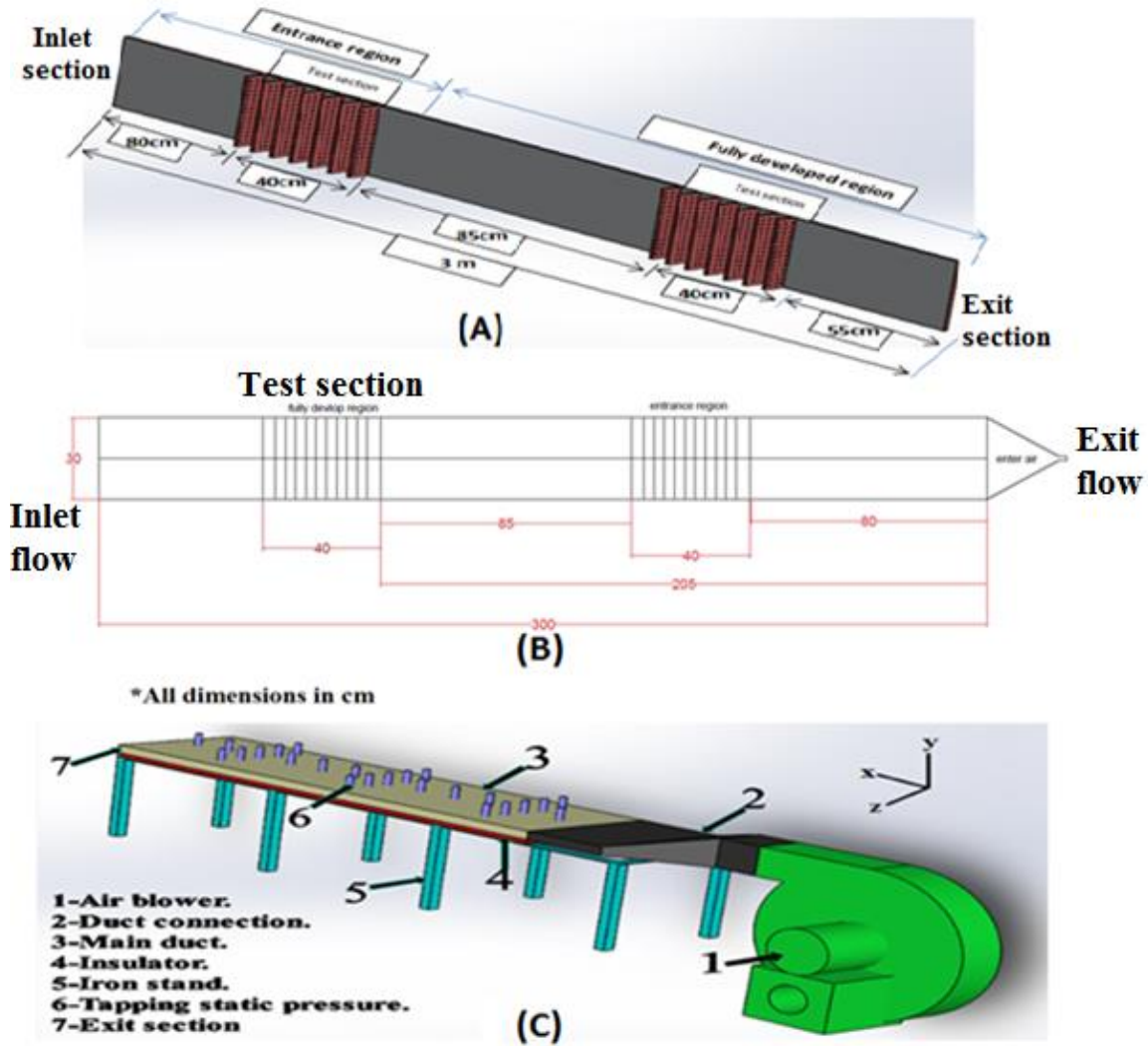


Fig (1) A, B, C The schematic of experimental set up

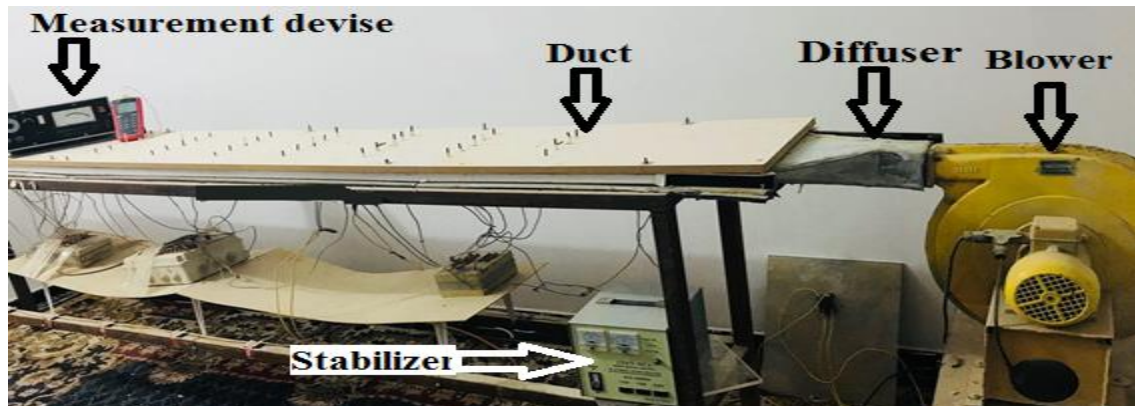


Fig. (2) Photograph of the experimental set up

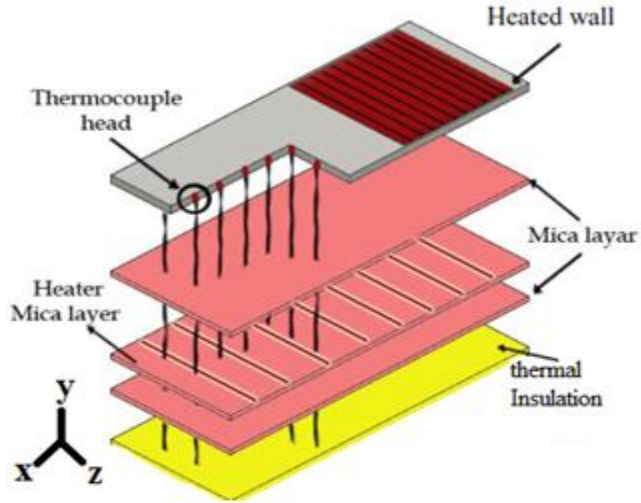


Fig. (3) Assembly of heater plate and heated wall



Fig. (4) Distribution of mesh wire in the test section

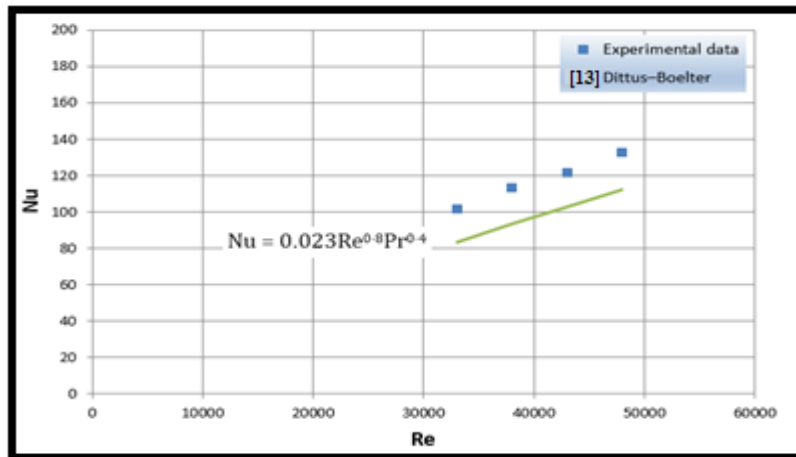


Fig. (5) Comparison of experimental and estimated values of friction factor smooth duct

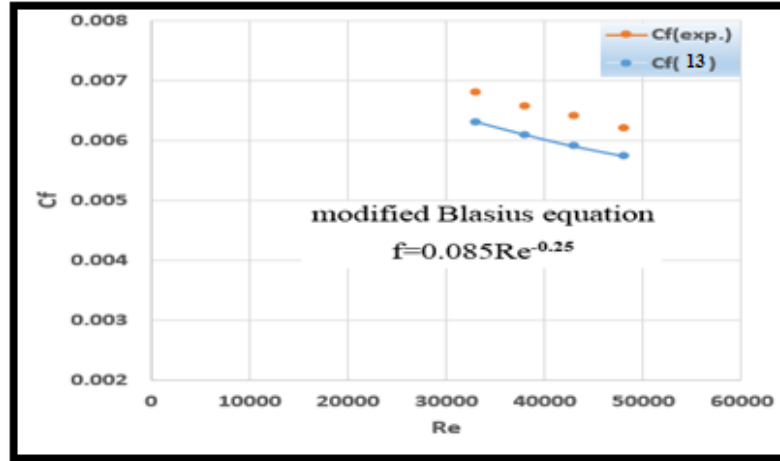


Fig. (6) Comparison of experimental and estimated values Cf smooth duct

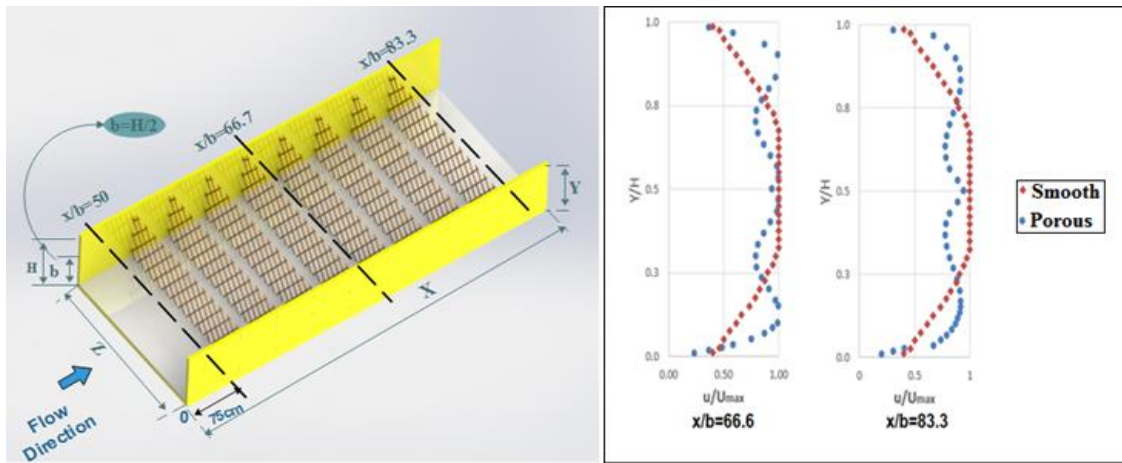


Fig (7) Dimensionless streamwise velocity profile in the entrance region for clear and porous cases (porosity=98% and  $R_p=1$ ) at  $Re = 4.8 \times 10^4$

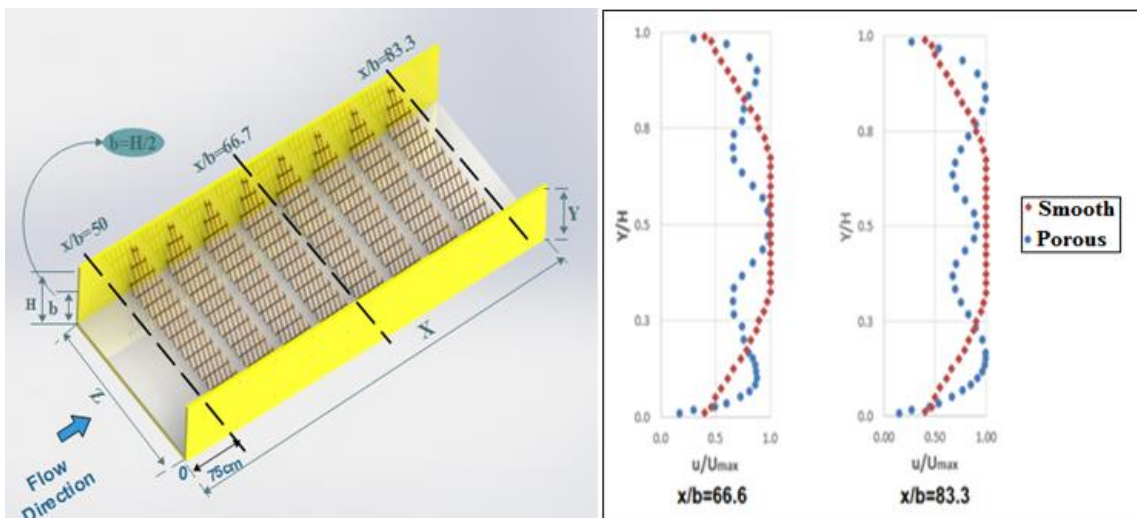


Fig (8) Dimensionless streamwise velocity profile in the entrance region for clear and porous cases (porosity=98% and  $R_p=1$ ) at  $Re=3.3 \times 10^4$

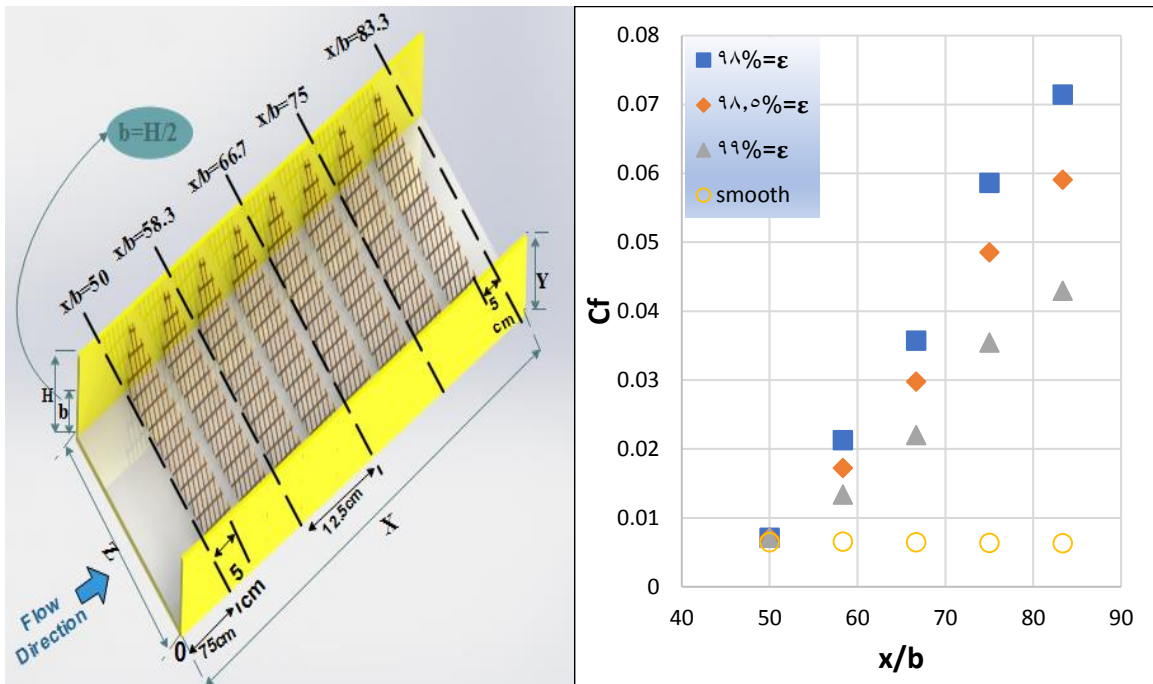


Fig (9) Distribution of local skin friction for smooth and porous media at entrance region of Reynolds number  $4.8 \times 10^4$  with  $R_p=1$  and different porosity values

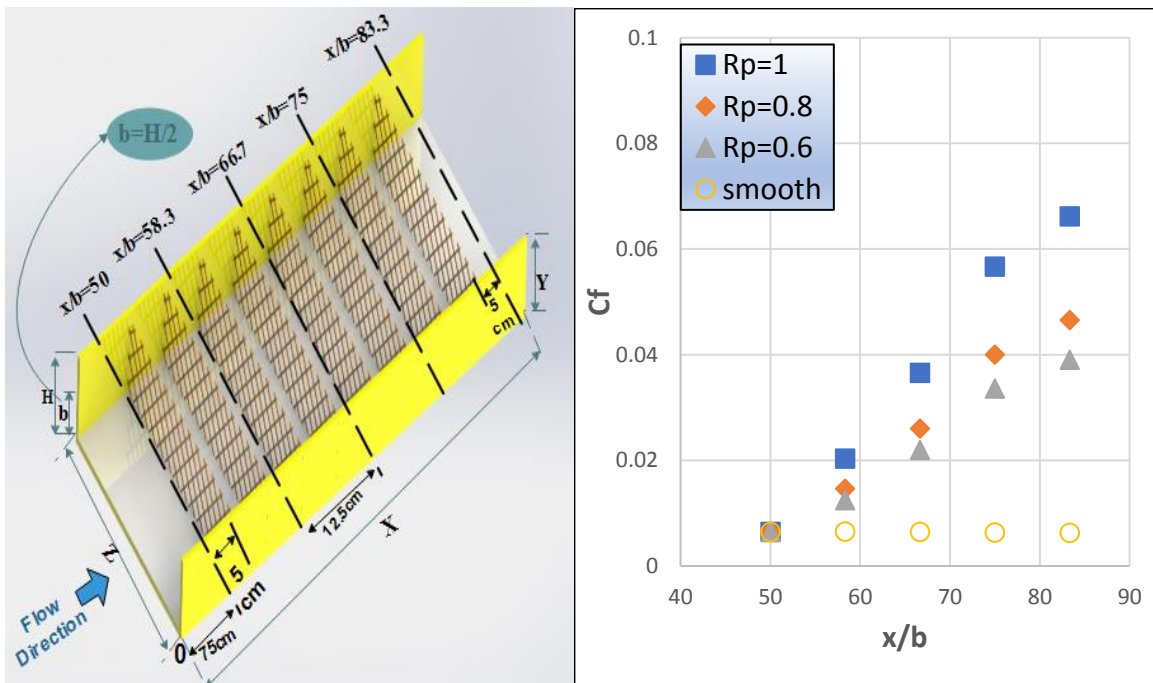


Fig (10) Distribution of local skin friction for smooth and porous media at entrance region of Reynolds number  $4.8 \times 10^4$  with  $\epsilon=98\%$  and different radius ratio.

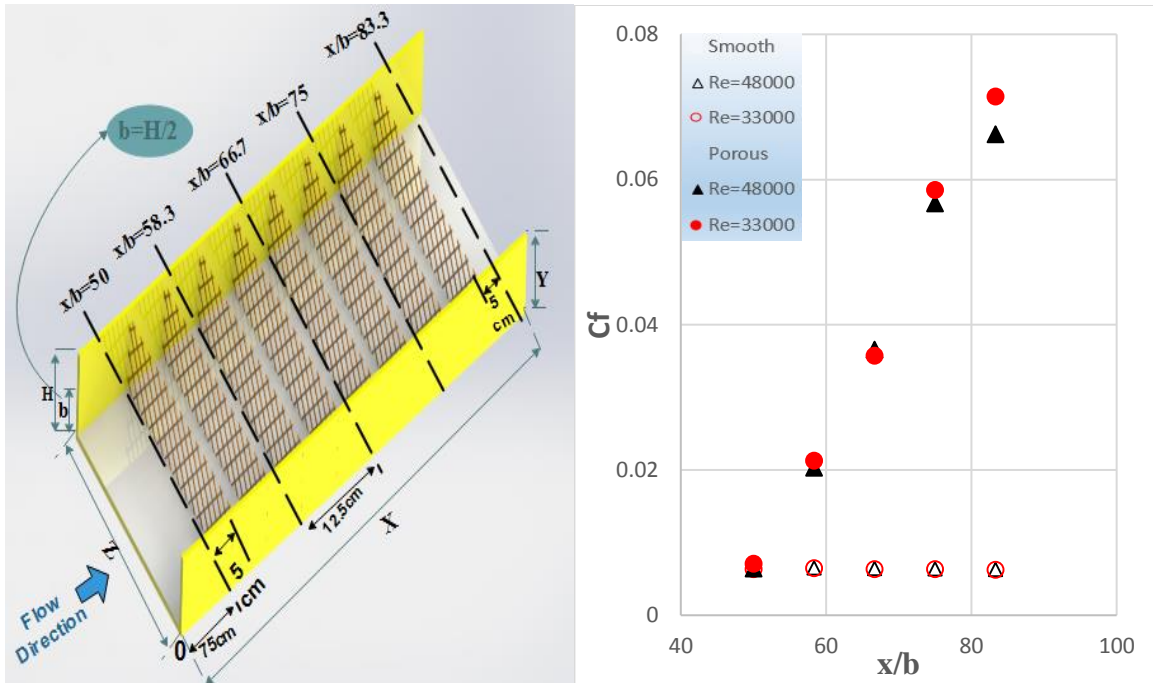


Fig (11) Variation of skin friction at different position in entrance region with  $Re_D=4.8 \times 10^4$  for smooth and porous media at porosity = 98% and  $R_p=1$

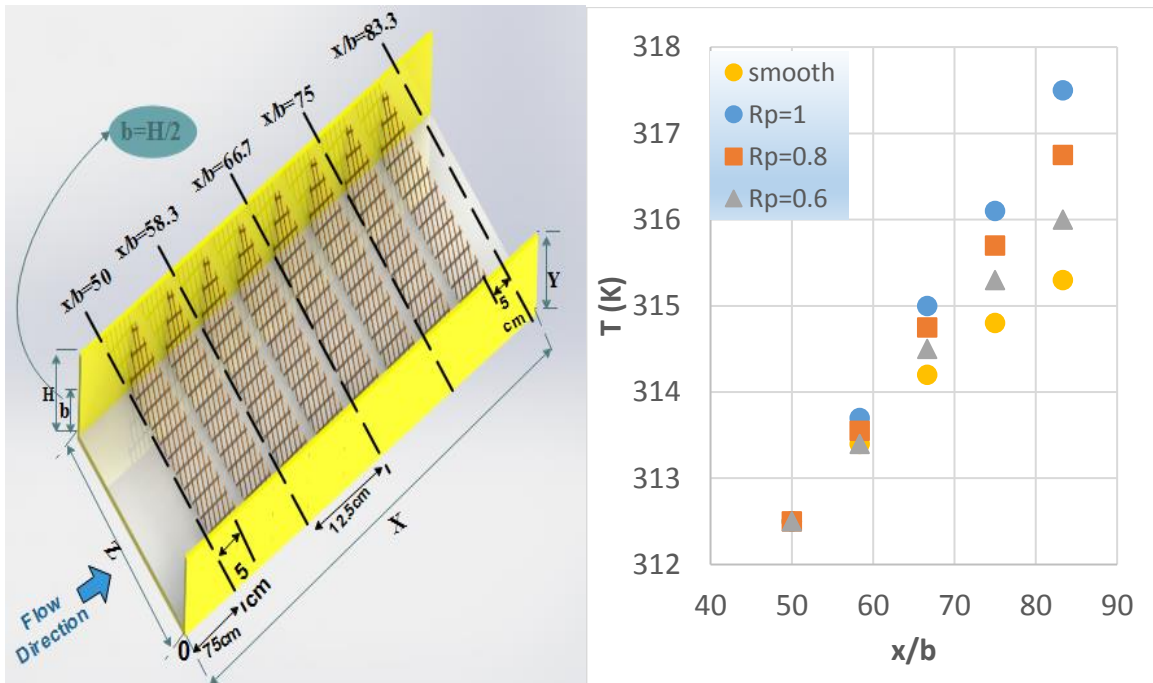


Fig (12) Variation of air temperature in streamwise direction for porous media at porosity=98%, Reynolds number  $4.8 \times 10^4$  and  $q=1833 \text{ w/m}^2$

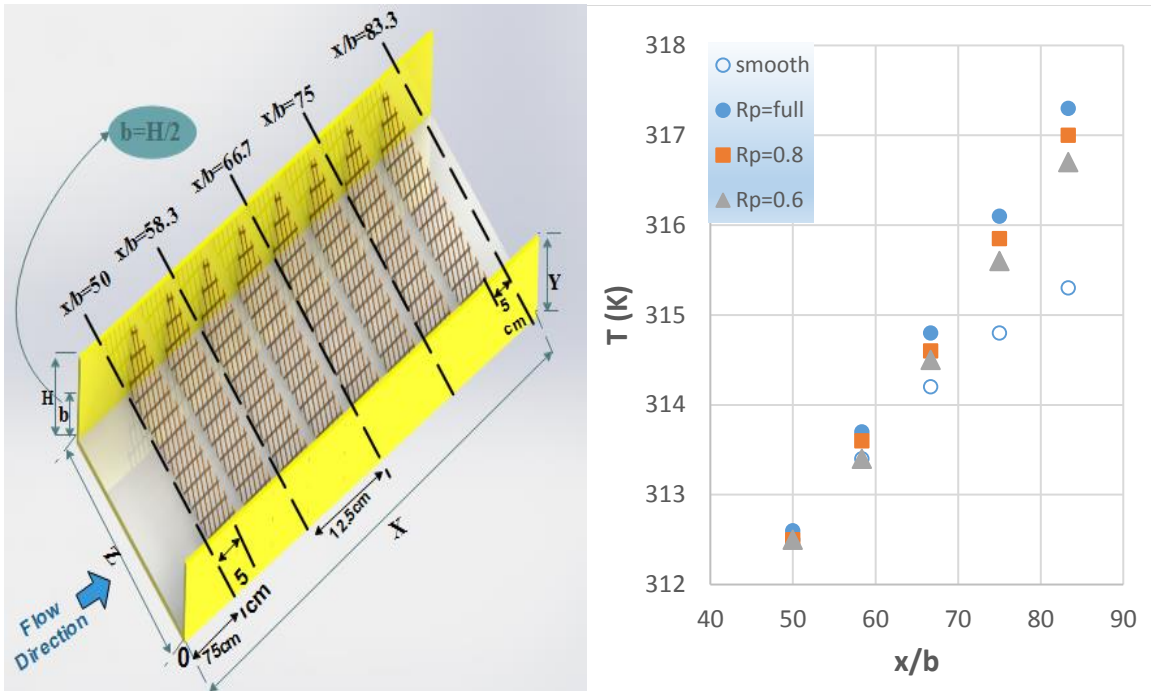


Fig (13) Variation of air temperature in streamwise direction for porous media with radius ratio at Reynolds number  $4.8 \times 10^4$ ,  $q=1833\text{ w/m}^2$  and  $\epsilon=98\%$

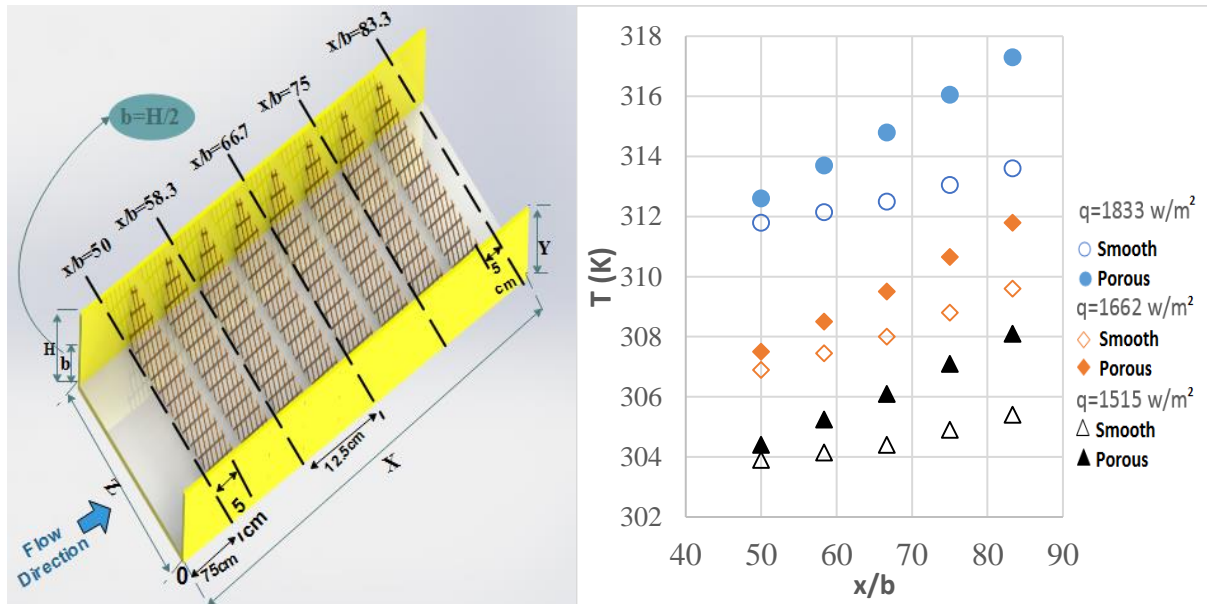


Fig (14) Variation of air temperature in streamwise direction for plain and porous media with heat flux at Reynolds number  $4.8 \times 10^4$ ,  $\epsilon=98\%$  and  $R_p=1$

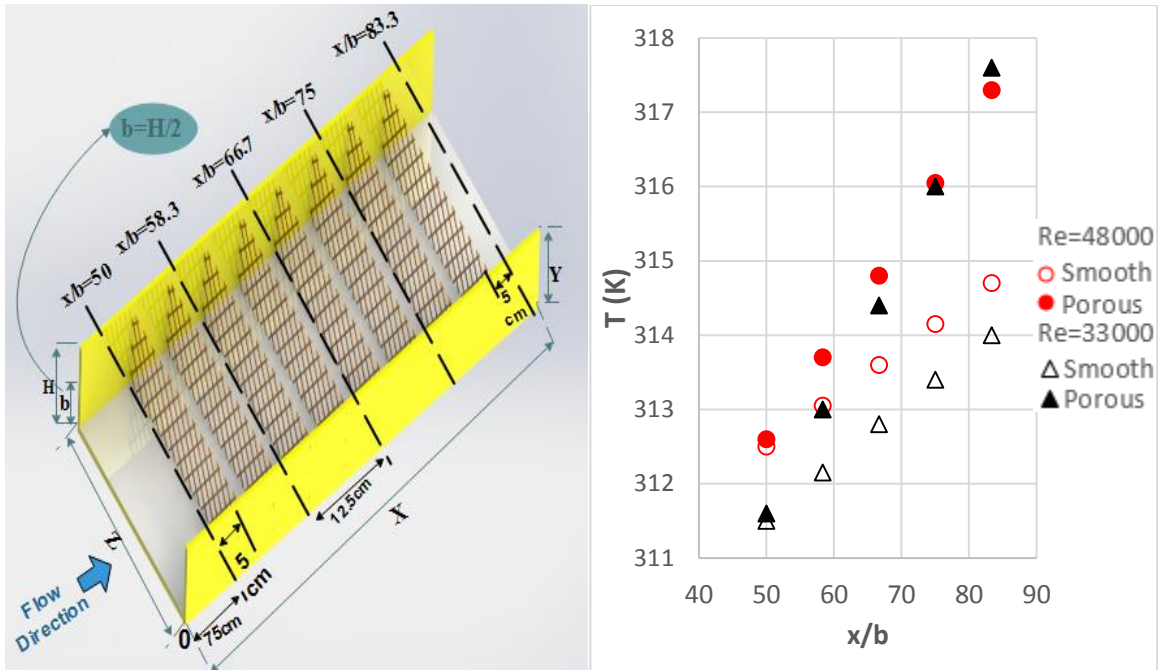


Fig (15) Variation of air temperature in streamwise direction for plain and porous media with Reynolds number  $4.8 \times 10^4$  at  $q = 1833 \text{ w/m}^2$ ,  $\epsilon = 98\%$  and  $R_p = 1$

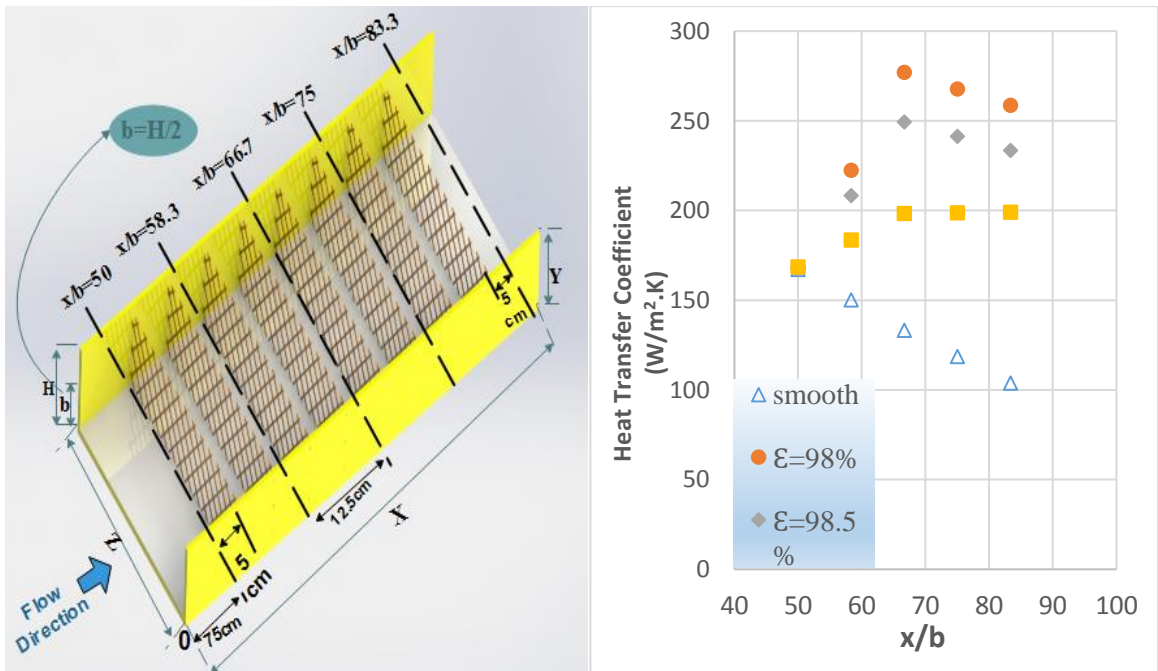


Fig (16) Variation of local heat transfer coefficient for porous media with porosity at Reynolds number  $4.8 \times 10^4$ ,  $q = 1833 \text{ w/m}^2$  and  $R_p = 1$

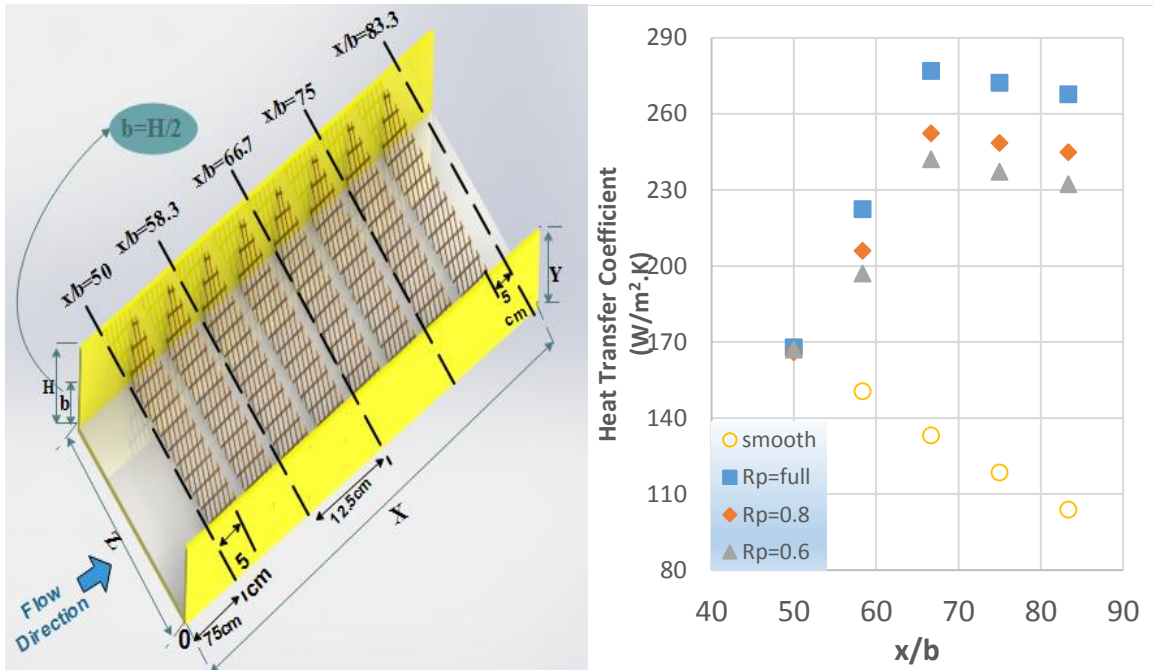


Fig (17) Variation of local heat transfer coefficient for plain and porous cases with radius ratio at Reynolds number  $4.8 \times 10^4$ ,  $q = 1833 \text{ w/m}^2$  and  $\epsilon = 98\%$

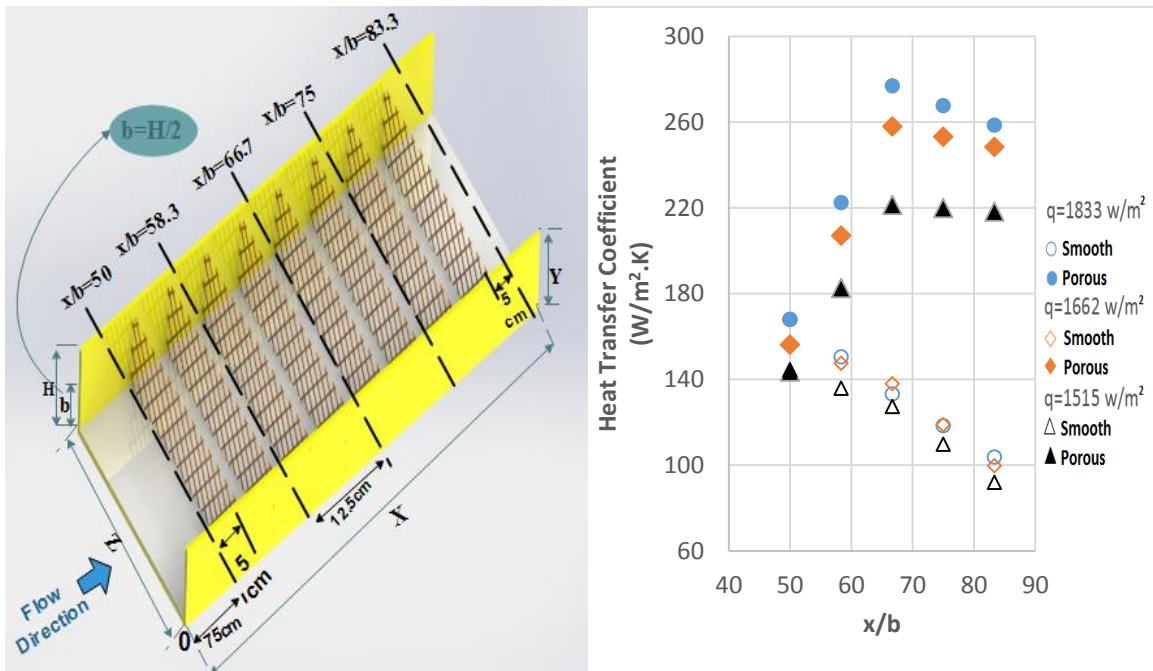


Fig (18) Variation of local heat transfer coefficient in streamwise direction for plain and porous media with heat flux at Reynolds number  $4.8 \times 10^4$ ,  $\epsilon = 98\%$  and  $R_p = 1$



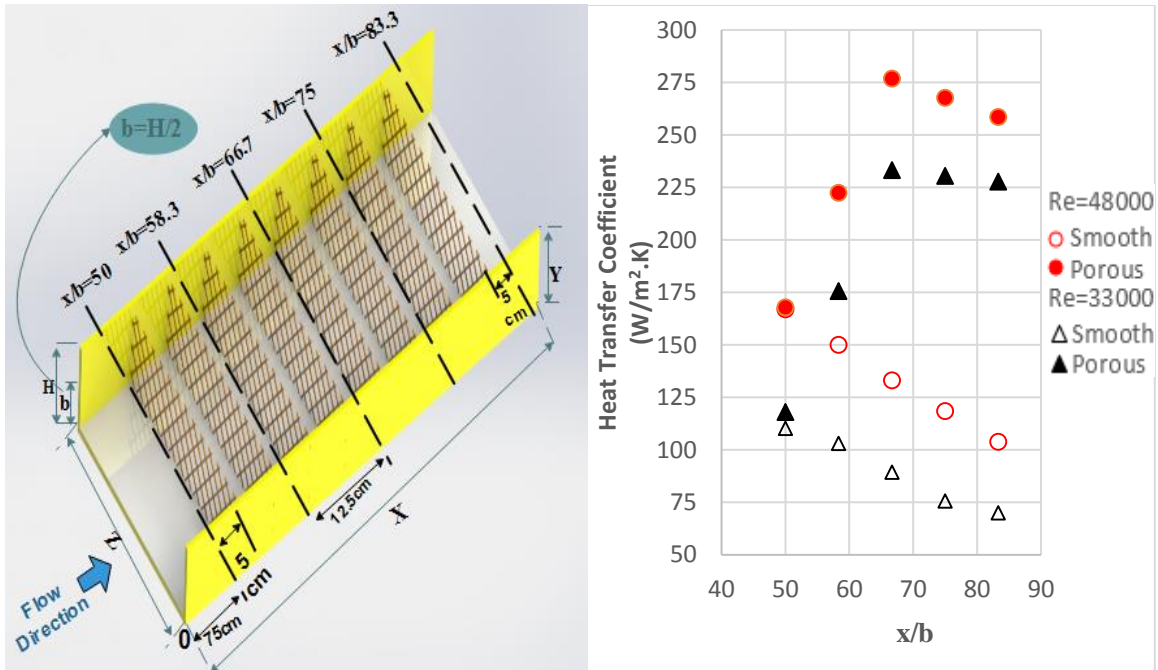


Fig (19) Variation of local heat transfer coefficient in streamwise direction for plain and porous media with  $Re_D$  at  $q=1833\text{ w/m}^2$ ,  $\epsilon=98\%$  and  $R_p=1$

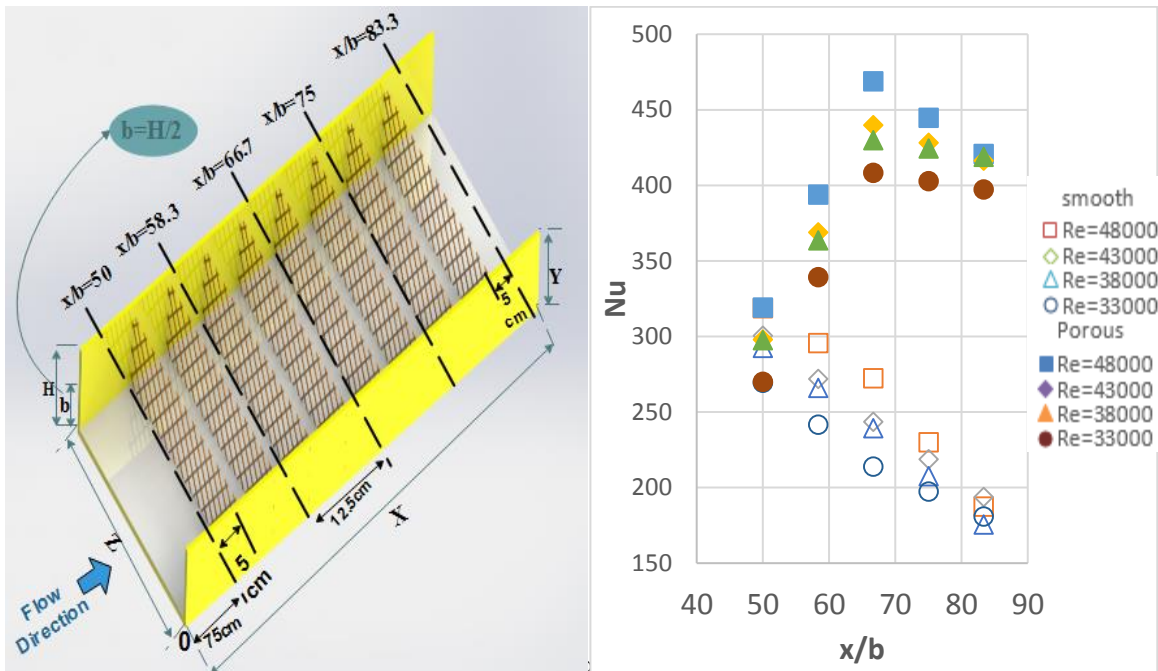
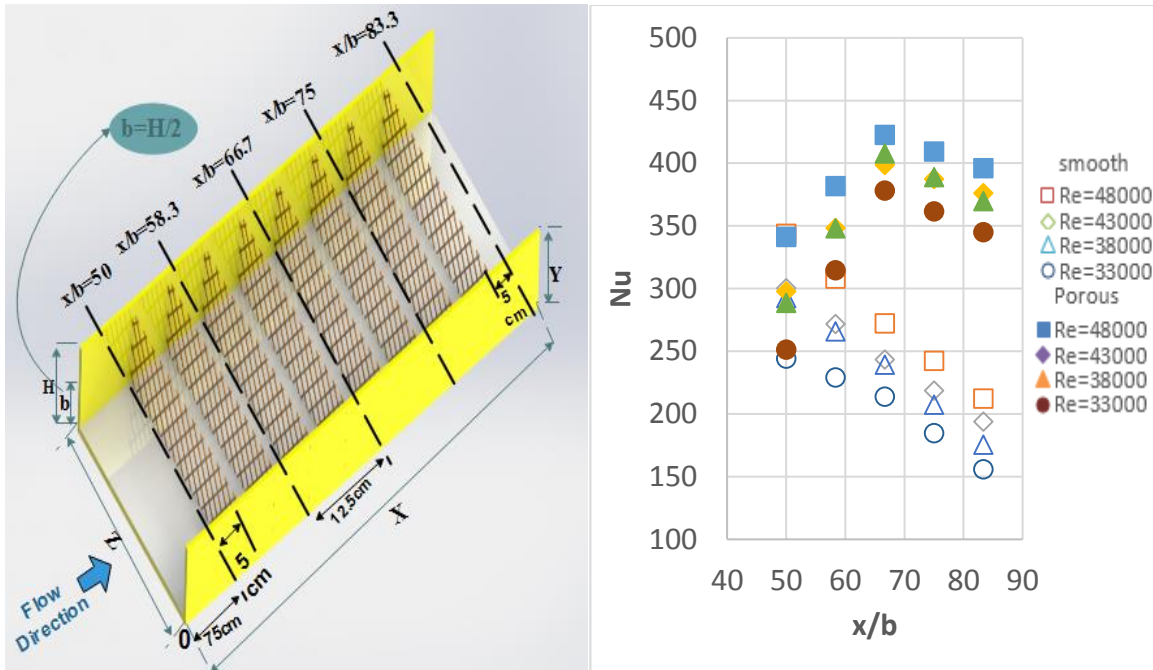
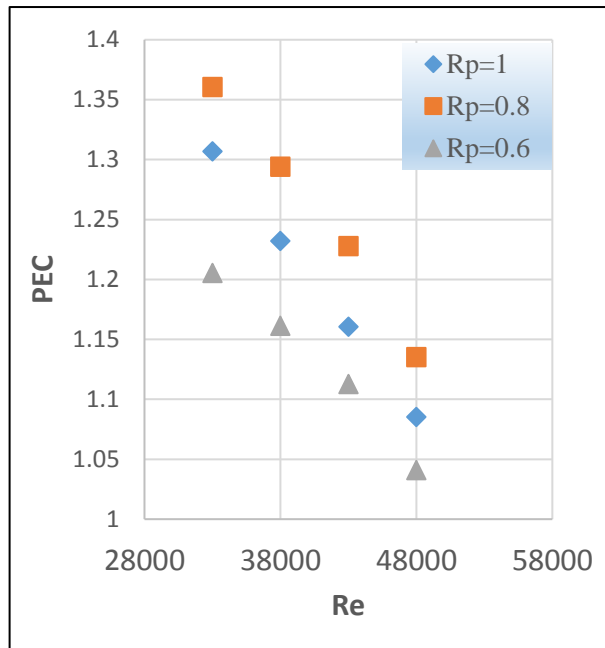


Fig (20) Variation of local Nusselt number for smooth and porous with  $Re_D$  at  $q=1833\text{ w/m}^2$ ,  $R_p=1$  and  $\epsilon=98\%$



**Fig (21) Variation of local Nusselt number for smooth and porous with  $Re_D$  at  $q=1833$   $w/m^2$ ,  $R_p=0.8$  and  $\epsilon=98\%$**



**Fig (22) Variation of thermal performance at entrance region with Reynolds number at  $q=1833$   $w/m^2$  and  $\epsilon=98\%$  and different radius ratio**

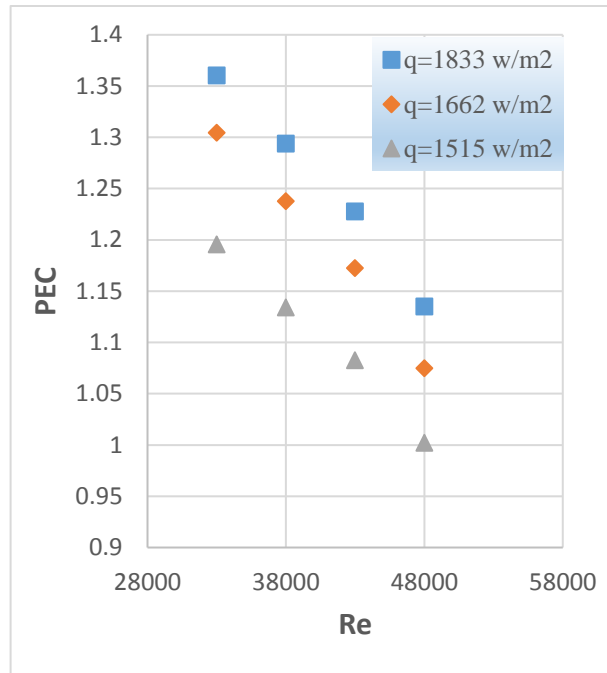


**Fig (23) Variation of thermal performance at entrance region with different Reynolds number  $q=1833 \text{ w/m}^2$ ,  $R_p=0.8$  and different  $\epsilon$  values**

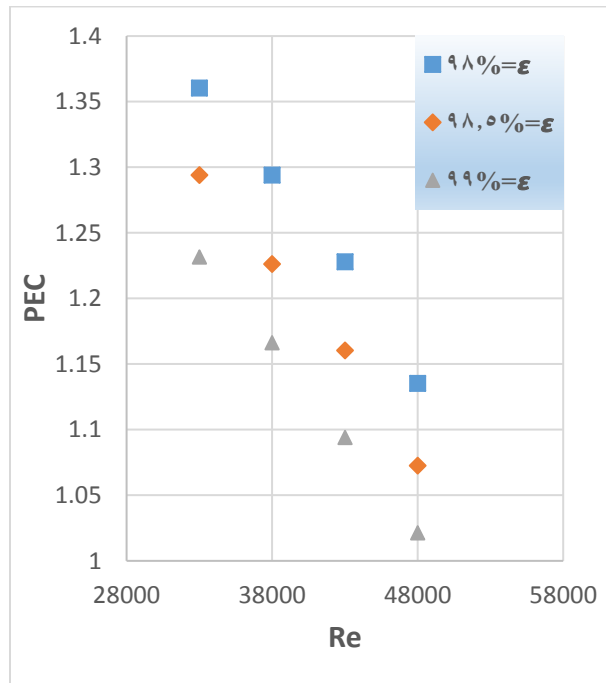


**Fig (24) Variation of thermal performance at entrance region with different Reynolds number  $\epsilon=98\%$ ,  $R_p=0.8$  and different heat flux values.**

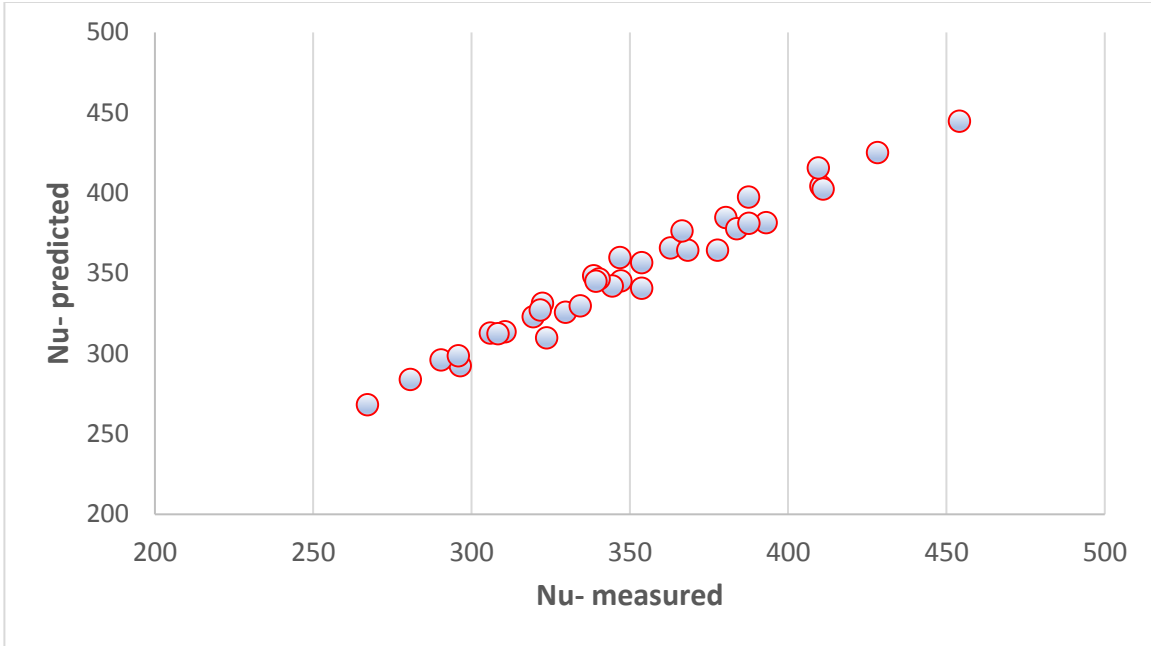


**Fig (25) Predicted data versus measured data for Nusselt number at entrance region.**

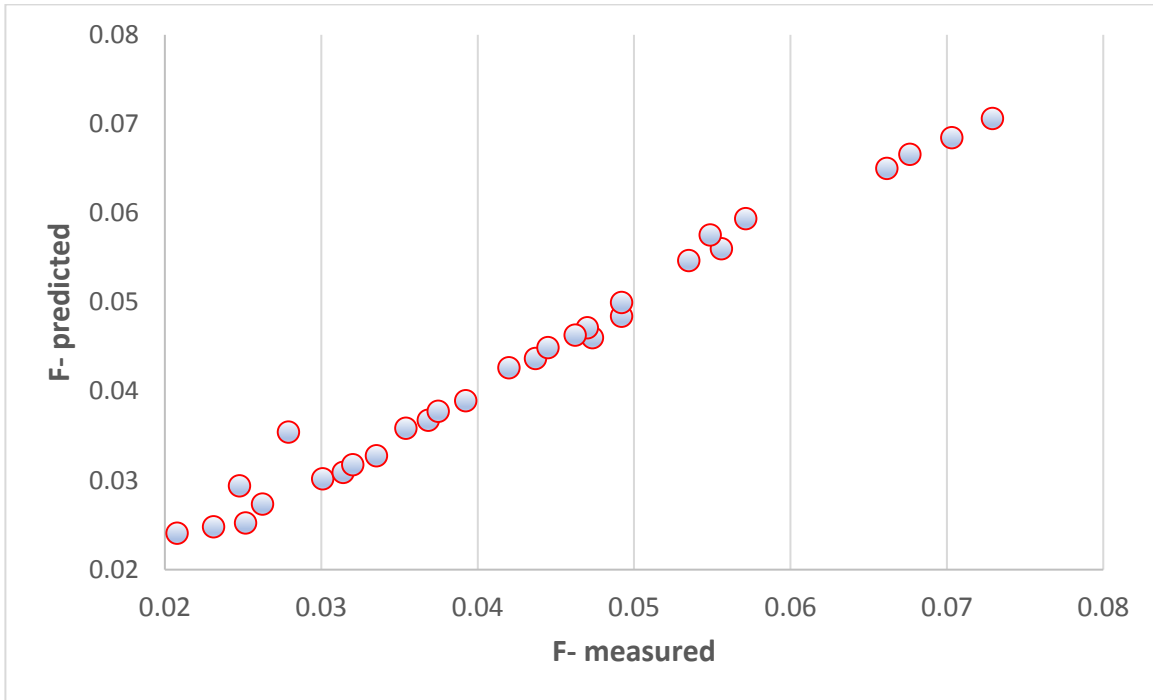


**Fig (26) Predicted data versus measured data for friction factor at entrance region.**

## انتقال الحرارة بالحمل القسري في وسط مسامي داخل قناة مستطيلة ضمن منطقة تطور الجريان

مؤيد رزوقي حسن      سهاد عبد الحميد      علي ناجح مهدي

قسم الهندسة الميكانيكية، الجامعة التكنولوجية، بغداد، العراق

[alinajeh999@gmail.com](mailto:alinajeh999@gmail.com)

[Sah\\_Jumaily66@yahoo.com](mailto:Sah_Jumaily66@yahoo.com)

### الخلاصة:

يعرض هذا العمل بحثاً تجريبياً عن خصائص التدفق وانتقال الحرارة في منطقة تطور الجريان عندما يكون الجريان مضطرباً في قناة مستطيلة محشوة بوسط مسامي وباستخدام الهواء كمائع عامل. عرضت القناة المستطيلة ( $300 \times 30$  مم) مع القطر الهيدروليكي (54.54 ملم) إلى تدفق مستمر للحرارة من السطح السفلي ( $1.5 \times 10^2 - 1.8 \times 10^2$  واط/م<sup>2</sup>) وتراوح أرقام رينولدز ( $3.3 \times 10^4 - 4.8 \times 10^4$ ). تم استخدام شبكة نحاسية بقطر (54.4 ملم) كوسط مسامي ولمسافات مختلفة (10, 15, 20 ملم) للعمل ضمن مدى المسامية (0.99 إلى 0.98). أثناء اجراء التجارب العملية، وتم دراسة تأثير نسبة ارتفاع المسامية (كون التعبئة كاملة وجزئية). كما بينت النتائج العملية ان استخدام الوسط المسامي يحسن انتقال الحرارة بمقدار (2.2) مرة مصحوب بزيادة من معامل الاحتكاك بمقدار (5) مرات. تم استنتاج العلاقات الرياضية لقيم عدد نسلت وعامل الاحتكاك في حالة استخدام الشبكة المسامية من النتائج المستحصل عليها.

**الكلمات الداله:** حمل قسري، المادة المسامية، شبكة سلكية، عدد نسلت، عامل الاحتكاك.